A Two-Tier Comparison Study of Three MPPT Control Algorithms for a PV-Powered Smart Greenhouse

Omrane Bouketir[1,2,*], LazharRahmani[1,3]
[1]*Department of Electrical Engineering, Faculty of Technology, Ferhat Abbas University, Almaabouda Campus, Setif 19137, Algeria*
[2]*Mechatronics Laboratory, Ferhat Abbas University, El Bez Campus, Algiers Road, Setif 19137, Algeria*
[3]*Automatic and System Laboratory, Faculty of Technology, Ferhat Abbas University, Almaabouda Campus, Setif 19137, Algeria*
[*]*omrane@univ-setif.dz; lazhar-rah@univ-setif.dz*

***Abstract*—In this research work, three maximum power point tracking (MPPT) control algorithms based on power feedback are applied to two types of converters, namely Zeta and buck-boost, in the photovoltaic (PV) system. The PV system is intended to guarantee the power supply to a remote smart greenhouse. The control algorithms investigated are perturb and observe (P&O), incremental conductance (IncCond), and fuzzy logic (FLC) methods. Their performance are investigated and compared for each converter. It is found that the maximum power is always achieved, even during abrupt changes in irradiation or/and in temperature. The three methods have shown to have good performance; fast response time and very low steady-state error, with minor preference of the P&O method where the output voltage followed the input with high efficiency. The comparative study revealed that the power response time of the PV generator under stable conditions (constant irradiance and constant temperature) for P&O and IncCond was longer in the buck-boost converter than in the Zeta. On the other hand, the ripple level was better for the buck-boost. For the FLC, the maximum power was reached in a shorter time (short response time) with the smallest ripple. As for operation under variable environmental conditions, the Zeta outperformed the buck-boost for each control technique.**

***Index Terms*—DC-DC power converters; Fuzzy logic; Maximum power point trackers; Photovaltaic systems.**

I. INTRODUCTION

Algeria, due to its geographical location, benefits from favourable conditions for the use of renewable energy, in particular solar energy. One of the possibilities of exploiting solar energy is its direct transformation into electric energy using photovoltaic (PV) converters [1]. Hence, Algeria is one of the countries that have very large solar energy potentials. In addition to its vast south Sahara area, which is sunny almost all year, its northern area experiences a long period of sunny days, especially from March to October with acceptable operating temperature. Government policies have been encouraging investment in solar energy and R&D in this field since the 1980s.

Manuscript received 3 April, 2024; accepted 12 May, 2024.

Powering a sizeable remote smart greenhouse using a PV generator is a great advantage in terms of writing off many expenses that should be endured when connecting the remote area to the public grid. Greenhouses require electric power to heat, cool, ventilate, and control humidity to maintain optimal growing conditions for crops. The amount of energy needed for climate control depends on factors such as outside temperature, sunlight levels, and desired internal conditions [2]. Some crops need additional lighting to extend daylight hours or provide consistent light levels, especially in regions with limited sunlight or during certain times of the year. The energy consumption for lighting can be significant, particularly if high-intensity artificial lighting systems are employed. Electric pumps may be used to deliver water to plants through irrigation systems [3], [4]. The energy consumption for irrigation depends on factors such as the size of the greenhouse, the water requirements of the crops, and the efficiency of the irrigation system.

Greenhouses equipped with automated systems for climate control, irrigation, and other functions can consume more energy due to the operation of sensors, actuators, and control systems [5]–[7]. Electric power may also be used to operate equipment and machinery, such as fans, motors, and conveyor belts, for tasks such as moving materials, harvesting, and packaging; in such a case, integration of multiple renewable energy sources is a requirement. This study limits its scope to the use of only a solar source.

However, exploitation of solar energy requires high investments, including extensive scientific research and maintenance costs, to achieve acceptable system efficiency. The development of suitable control strategies and algorithms together with a novel system design are among key elements toward achieving such good efficiency.

For the PV system to be efficient, a competent maximum power point tracking (MPPT) technique is necessary to predict and track the MPP regardless of weather conditions and to set the operating point of the PV installation at this point.

Various MPPT techniques have been proposed to improve

the efficiency of a PV system. Some of them focus on the improvement of MPPTs under uniform irradiance, and others on the development of MPPTs under nonuniform irradiance [8]. A comprehensive summary of these techniques under the two conditions can be found in [9]. Perturb and observe (P&O) technique is an online algorithm used under uniform irradiation conditions. It is commonly used due to its simplicity when it is implemented. This algorithm senses the output voltage of the PV array and then perturbs it by a small change (either increase or decrease). This perturbation results in a change in output power that is then compared with successive perturbing cycles [10]–[12]. The incremental conductance algorithm (IncCond) is also an online technique used under uniform conditions where the slope of the P-V curve is detected and the MPP is traced by looking for the peak of the P-V curve [13]–[17].

The choice of DC-DC converter for PV systems plays an important role in improving efficiency. Various DC-DC converters in the PV system are analysed throughout the PV literature works [18]–[24]. From previous research, it is obvious that each converter has its own advantages and disadvantages. Therefore, it is essential to design a PV system that has the ability to produce maximum efficiency and the smallest possible ripple under minimum stress.

This paper considers the use of two power converters, namely Zeta converter and buck-boost converter powered by a photovoltaic module as the input energy source. A Zeta converter is a fourth-order DC-DC converter composed of two inductors and two capacitors and is capable of operating in step-up or step-down modes. The proposed system consists of a solar panel, a DC-DC converter, and an MPPT controller. The MPPT is carried out using P&O and then using an incremental conduction method. A fuzzy logic-based algorithm was also considered for the purpose of performance comparison. The P&O is popular and most commonly used in practice due to its simplicity and the ease of implementation, the incremental conduction method.

The same three MPPT methods are also applied to the buck-boost converter powered by the same PV generator as above. The performance of each algorithm is compared for each converter. A global comparison of the performance is then carried out between the two systems considering the performance of the three techniques on the two converters when applied to the designated smart greenhouse.

II. SYSTEM DESIGN

A. Greenhouse Prototype

In addition to the main systems that consume energy (irrigation system, heating and cooling systems, lighting systems, fogging system, and CO_2 generator), a smart greenhouse also includes sensors and Internet of things (IoT) devices that consume electric power as well. All growing phases of crops can be modified by the control of temperature, humidity, light, and CO_2 in a greenhouse, making climate control in greenhouses a multivariable problem. The energy consumed by these equipments accounts for more than 90 % of the total energy consumed in the greenhouse. The other remaining 10 % is consumed by the electronic sensors and controlling devices for the different actuators [25]–[27]. The total power consumption of a smart greenhouse depends mainly on its size and the crops it grows in addition to the surrounding weather. In this paper, an amount of 400 W is deemed as a mean value for the greenhouse prototype considered for study purpose. This power is assured by five PV generators (PVGs), as discussed in the following.

B. PV Generator Characteristics

The power required by the smart greenhouse prototype is met by installing five similar PV generators (PVGs), each of which has the characteristics listed in Table I.

TABLE I. CHARACTERISTICS OF THE STUDIED PVG.

Parameter	Value
Type	Suntech 85 W
Number of Series Cell, Ns	36
Standard Insolation, E_{ref}	1000 W/m^2
Reference Ambient Temperature, T_{ref}	45 °C
Maximum Power, P_{max}	85.2 W
Max Power Point Voltage, V_{mpp}	17.60 V
Max Power Point Current, I_{mpp}	4.83 A
Open Circuit Voltage, V_{OC}	21.9 V
Short Circuit Current, I_{SC}	5.15 A
Series Resistance, R_s	0.145 Ω
Parallel Resistance, R_p	300 Ω

In a PV system, the input energy source is energy with virtually zero operating cost. It operates quietly with no emissions, even as the load increases. Thanks to recent developments, solar energy systems are readily available for industrial and domestic use with the added benefit of minimal maintenance.

However, the output power induced in the photovoltaic modules depends on solar irradiation and temperature. Photovoltaic modules have very low conversion efficiency, on the order of 15 % for manufactured modules. In addition, due to variations in temperature, radiation, and load, this efficiency can be greatly reduced. In fact, the efficiency of any semiconductor device decreases sharply with increasing temperature.

III. MATERIALS AND METHODOLOGY

The solar cell, round or square in shape, is the basic element of a solar system. A set of cells forms a solar module; in a module the cells are electrically connected to each other and encapsulated, therefore, protected from external agents. Several modules form a solar panel. Several panels form a system or solar field, to which are added protections, a regulator, an energy storage system (e.g., battery), control and measuring devices, and an inverter.

The mathematical model for the current-voltage characteristic of a PV cell is given by

$$\boldsymbol{I_{pv} = I_{ph} - I_{sat}\left[e^{\left(\frac{q\left(V_{pv}+\left(I_{pv}\times R_s\right)\right)}{n\times K\times T}\right)} - 1\right] - \frac{V_{pv}+\left(I_{pv}\times R_s\right)}{R_{sh}}}, \quad (1)$$

where $\boldsymbol{I_{sat}}$ is the saturation current, $\boldsymbol{K}$ is the Boltzmann constant ($\boldsymbol{K = 1.381 \times 10^{-23}}$ $\left[\frac{J}{K}\right]$), $\boldsymbol{T}$ is the temperature of the

PV cell in Kelvin ($[K]$), q is the electron charge ($q = 1.6 \times 10^{-19}$ $[C]$), n is the ideality factor of the junction ($1 < n < 3$), here taken as $n = 1.6$, I_{pv} is the current supplied by the cell when it operates as a generator, V_{pv} is the voltage across the same cell, I_{ph} is the photocurrent of the cell depending on the insolation and the temperature, R_{sh} is the Shunt resistance, it models the leakage currents of the junction, R_s is the series resistance representing the various contact and connection resistances; I_{ph} is the photon current which depends on the temperature and the sunshine as given by the equation

$$I_{ph} = \left[I_{cc} + K_i \left(T - T_{ref} \right) \right] \times \frac{E}{1000}, \tag{2}$$

where I_{ph} is computed in the standard conditions (25 °$[C]$, $1000 \left[\frac{W}{m^2} \right]$), K_i is the ratio between the short circuit current and the temperature coefficient (0.0017 $[A/K]$), T_{ref} is the reference temperature, 25 °$[C]$ = 298 °$[K]$, E is the solar irradiance in $\left[\frac{W}{m^2} \right]$, I_{cc} is the short circuit current in $[A]$; I_{sat} is the saturation current in $[A]$ expressed by

$$I_{sat} = I_{rs} \times \left[\frac{T}{T_{ref}} \right]^3 \times exp \left[\frac{q \times E_g}{n \times K} \times \left(\frac{1}{T_{ref}} - \frac{1}{T} \right) \right], \tag{3}$$

where E_g is the gap energy of the semiconductor used ($E_g \approx 1.1\,eV$ for the polycrystalline silicon at 25 °C]), and I_{rs} is the inverse saturation current in $[A]$ given by

$$I_{rs} = \frac{I_{cc}}{\left[exp\left(q \times V_{oc} / K \times n \times T \right) - 1 \right]}. \tag{4}$$

A. *Shading Effect*

To take into account the shading effect, the PV module (Suntech 85 W) of 36 cells was divided into three parts of 12 cells, each behaves as a single module. The series and shunt resistances of each part are taken equal to 1/3 of the corresponding value for the complete module. Figure 1 illustrates the algorithm implemented to draw the P-V characteristics under partial shading of each submodule. The resulting curves are depicted in Fig. 2. Three models are distinguished as follows.

Model 1: The global maximum power point (GMPP) is located to the left of the P-V curve (Fig. 2(a)). In this case, the insolation of the first panel is set to 1000 W/m² (not shaded), the second to 500 W/m², and the third to 600 W/m² (both partially shaded).

Model 2: The GMPP is located in the middle of the P-V curve (Fig. 2(b)). In this case, the insolation of the first panel is set to 600 W/m², the second to 900 W/m², and the third to 200 W/m² (all panels are considered shaded with different extents).

Model 3: The GMPP is located to the right of the P-V curve (Fig. 2(c)). In this case, the insolation of the first panel is set to 200 W/m², the second to 400 W/m², and the third to 1000 W/m².

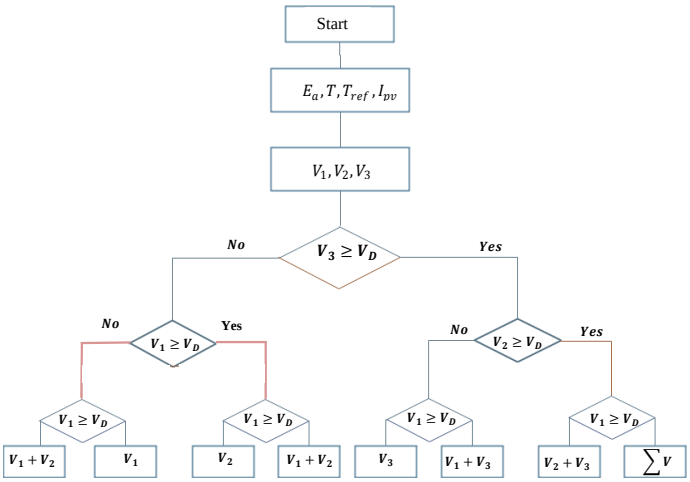

Fig. 1. Flowchart of the algorithm for plotting the I-V curves under partial shading.

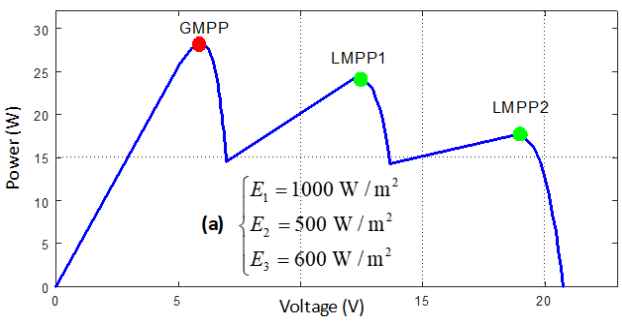

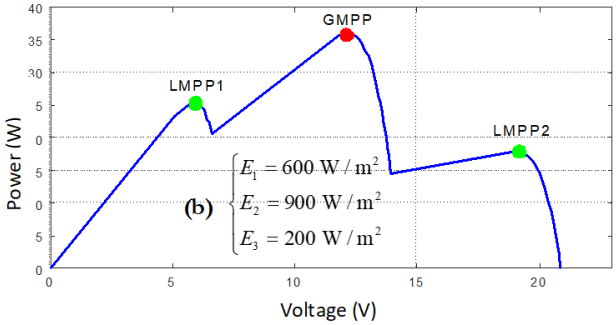

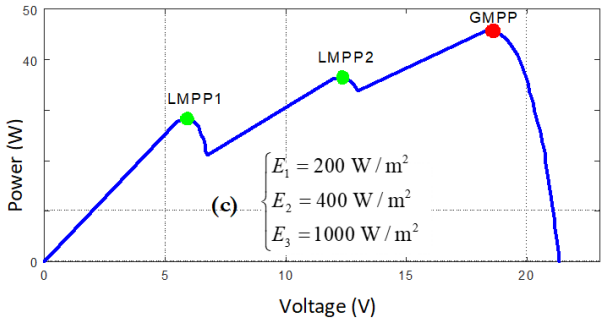

Fig. 2. P-V curves of three panels connected in series under partial shading: (a) GMPP on the left; (b) GMPP in the middle; (c) GMPP on the right.

B. *Load Adaptation Stage*

Due to the variations in temperature, radiation, and load, PV efficiency can be significantly reduced. In fact, the efficiency of any semiconductor device decreases sharply with temperature. To ensure that photovoltaic modules always provide the maximum possible power under uniform climatic operating conditions, an MPPT control algorithm is implemented.

Currently, there are still many applications in which a direct connection is made between a PV generator and a load [28], [29]. This choice is mainly related to the simplicity of the operation and the very high degree of reliability, owing to the absence of electronics, and its low cost. However, the disadvantage of this configuration is that the transfer of the maximum power available at the PV module terminals to the load is not guaranteed.

To extract the MPP available at all times at the PV generator terminals and transfer it to the load, an adaptation stage is used between the PV generator and the load as depicted in Fig. 3. This stage plays the role of an interface between the two devices by ensuring, through a control action, the transfer of the maximum power supplied by the generator so that it is as close as possible to the maximum power available. These impedance adapters are DC-DC converters controlled by a suitable control algorithm.

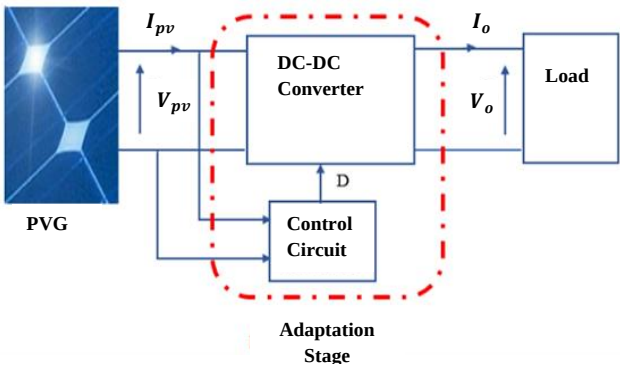

Fig. 3. Diagram of an adaptation interface.

C. *Static Converters*

Besides the inverse polarity of the output voltage of the buck-boost converter, the main issue is the discontinuity of its input current because the semiconductor switch is in series with the energy source (Fig. 4). Large LC filters are required to mitigate the problems such as high ripples and large number of current harmonics caused by this discontinuity. Still, this low-cost converter is easy to implement, because it has only an inductor and capacitor as energy storage devices.

However, the Zeta converter is a capacitive storage DC-DC power converter that realises the Buck and Boost functions, but it is nonpolarity inverting. The basic electric circuit of this converter is shown in Fig. 5.

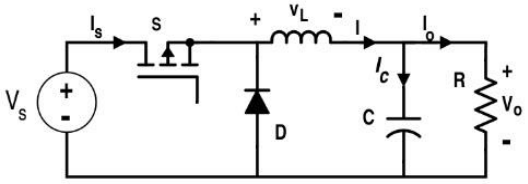

Fig. 4. Circuit diagram of conventional buck-boost converter.

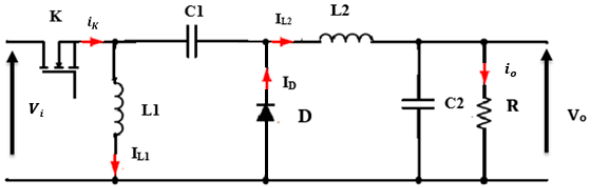

Fig. 5. Electric circuit of the Zeta converter with a resistive load.

When this converter operates in a continuous conduction operating mode, there are two states during one switching period (T). The first is when the switch is on, and the other is when the switch is off. The Zeta converter consists of an IGBT transistor as a switch, a diode, two capacitors C1 and C2, and two inductors L2 and L2 with load R. The advantages and shortcomings of the Zeta converter are detailed in [30].

The Zeta converter parameters (L1, L2, C1, and C2) can be designed to operate in continuous conduction mode (CCM). The CCM mode always results in reduced stress on converter components. In addition, the CCM offers low ripples on the output side due to the presence of inductance L2. Therefore, better MPP results will be obtained.

The components of the Zeta converter are designed based on the following values for the continuous conduction mode: the input voltage V_i = 17.6 V; The output voltage V_o = 22 V, and switching frequency f = 2500 Hz.

Duty cycle D is calculated as

$$\boldsymbol{D = \frac{V_o}{V_o + V_i} = \frac{22}{22 + 17.6} \rightarrow D = 0.56,} \qquad \boldsymbol{L_1 = 0.039H,}$$

$\boldsymbol{L_2 = 0.039H,}$ $\boldsymbol{C_1 = 0.0017F}$, with ripples in inductors' current of 5 % and ripple in the capacitor voltage of 9 %. Capacitor C_2 is taken as 200 μF.

A simulation of the operation of this converter for two values of duty ratio (0.4 and 0.7) shows that in the steady state there are small ripples. For D = 0.4, the converter behaves as a buck converter, while for D = 0.7, the converter acts as a boost converter as shown in Fig. 6.

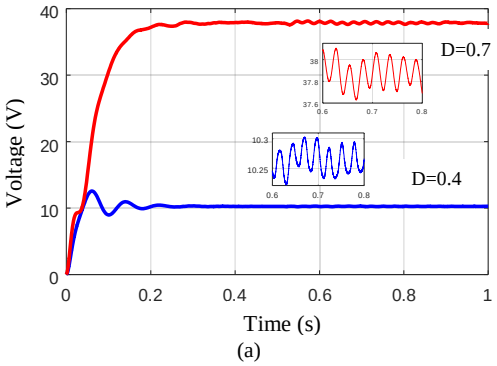

(a)

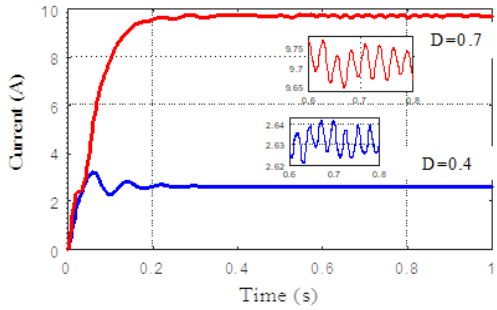

(b)

Fig. 6. (a) Output voltage and (b) Current of the Zeta converter for two values of duty ratio.

IV. Results of Applied MPPT Methods

For a given irradiation and temperature, there is an operating point where the power delivered is maximum. Optimisation consists of permanently pursuing this point by acting automatically on the load seen by the PV generator. This load adaptation, the principle of which is generally carried out using a static converter (Fig. 3), whose losses must be as low as possible and which can, moreover, ensure a shaping function of PVG output, different attitudes can be considered regarding the control of the adapter. This type of control is often called "Maximum Power Point Tracking" or MPPT in short.

The commonly used control technique consists of acting on the duty cycle automatically to bring the generator to its optimal operating value, regardless of weather instabilities or sudden load variations that can occur at any time [29].

For a variation in solar insolation, a simple readjust of the value of the duty cycle leads to convergence towards the new maximum power point MPP2 as in Fig. 7.

Several solutions have been proposed for the MPP search algorithm; here, three techniques, namely the perturbation & observation (P&O) algorithm, the incremental conductance algorithm (IncCond), and fuzzy logic control (FLC), are applied to two types of converters and their performances are compared.

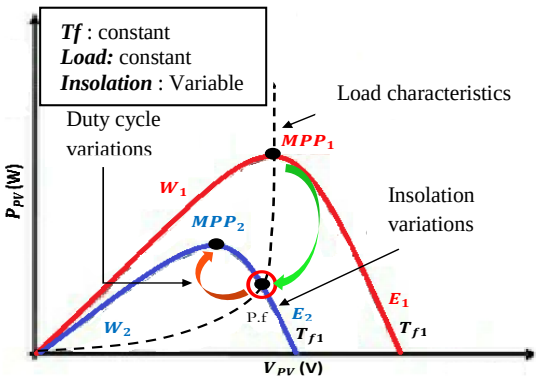

Fig. 7. Search and recovery of the maximum power point following a variation in solar radiation.

A. P&O Algorithm

It is a widely used method, simple in structure, easy to implement, and gives interesting results. Its principle is based on the disturbance of the operating point, increases and decreases the operating voltage, and its effect on the power (P) is observed.

If the power increases ($\Delta P > 0$), we are therefore in the right direction, we continue the disturbance in the same direction else ($\Delta P < 0$), so we move away from the MPP, and we reverse the disturbance. Figure 8 illustrates its operating principle.

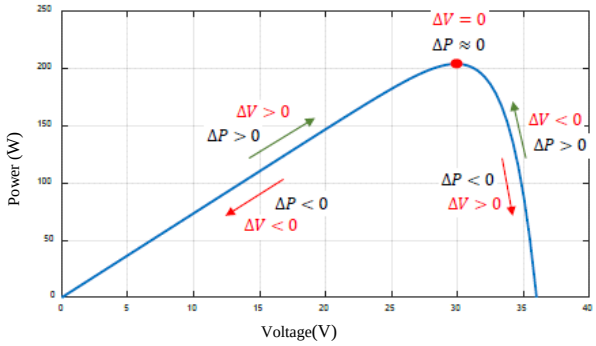

Fig. 8. Principle of MPPT with the *P&O* method.

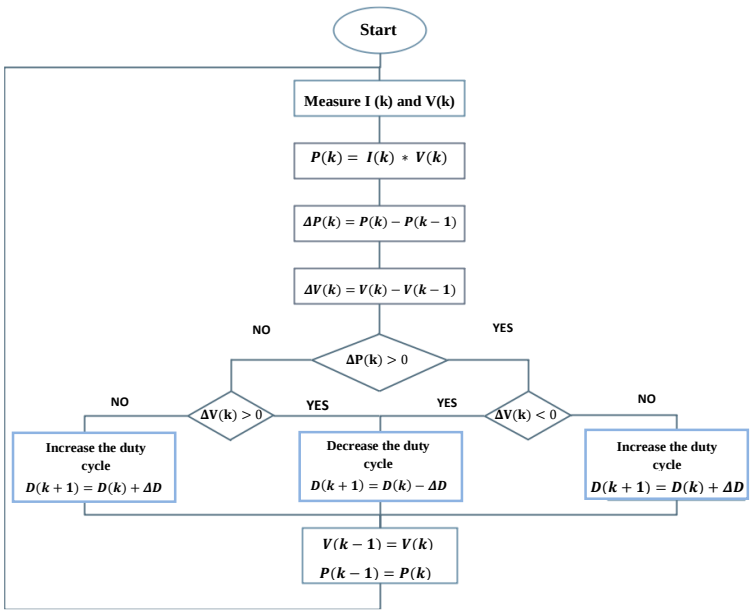

Fig. 9. Flowchart of the P&O MPPT method.

The flowchart of this method is given in Fig. 9.

The current and voltage of the PVG are measured, then the

power P(t) and the voltage variation (ΔV) are calculated. If the power has increased (ΔP > 0) we are therefore in the right direction, we continue thus to increase V (if ΔV > 0) or we continue to decrease it (if ΔV < 0). If the power has decreased (ΔP < 0) then it is necessary to reverse the process (i.e., increase V if ΔV < 0 and decrease if ΔV > 0).

B. *IncCond Algorithm*

It is a widely used method because it is not difficult to implement. It addresses the problem of the divergence of the P&O method in the case of a rapid change in the solar insolation. This method is based on the determination of the sign of the derivative of the power (slope), which does not change with the change of the insolation. Figure 10 illustrates its operation principle.

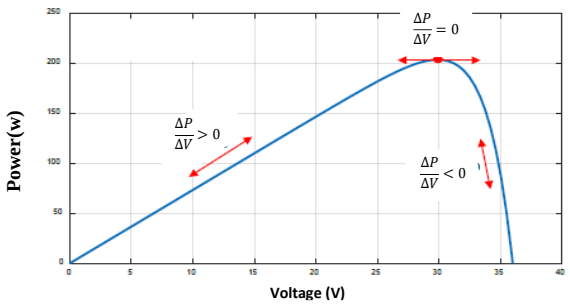

Fig. 10. Principle of MPPT with the IncCond method.

The variation of power as a function of voltage is given by

$$\frac{\Delta \mathbf{P}}{\Delta \mathbf{V}} = \frac{\Delta(\mathbf{I}.\mathbf{V})}{\Delta \mathbf{V}} = \mathbf{I}\frac{\Delta \mathbf{V}}{\Delta \mathbf{V}} + \mathbf{V}\frac{\Delta \mathbf{I}}{\Delta \mathbf{V}}. \quad (5)$$

Hence,

$$\frac{\Delta \mathbf{P}}{\Delta \mathbf{V}} = \mathbf{I} + \mathbf{V}\frac{\Delta \mathbf{I}}{\Delta \mathbf{V}} \frac{\Delta \mathbf{P}}{\Delta \mathbf{V}} = \frac{\Delta(\mathbf{I}.\mathbf{V})}{\Delta \mathbf{V}} = \mathbf{I}\frac{\Delta \mathbf{V}}{\Delta \mathbf{V}} + \mathbf{V}\frac{\Delta \mathbf{I}}{\Delta \mathbf{V}}. \quad (6)$$

At the point of maximum power, the derivative $\left(\frac{\Delta \mathbf{P}}{\Delta \mathbf{V}} = 0\right)$, which gives the

$$\frac{\Delta \mathbf{I}}{\Delta \mathbf{V}} = -\frac{\mathbf{I}}{\mathbf{V}}. \quad (7)$$

We notice that checking the sign of the slope amounts to comparing the conductance (I/V) and its increment $\left(\Delta I/\Delta V\right)$ as follows:

$\frac{\Delta P}{\Delta V} > 0 \Rightarrow \frac{\Delta I}{\Delta V} > -\frac{I}{V}$ to the left of the MPP (positive slope) $\longrightarrow$ action is to increase **V**;

$\frac{\Delta P}{\Delta V} < 0 \Rightarrow \frac{\Delta I}{\Delta V} < -\frac{I}{V}$ to the right of the MPP (negative slope) $\longrightarrow$ action is to decrease **V**;

$\frac{\Delta P}{\Delta V} = 0 \Rightarrow \frac{\Delta I}{\Delta V} = -\frac{I}{V}$ at the MPP, no action is required (the duty cycle remains constant).

Figure 11 shows the theoretical flowchart for implementing this method.

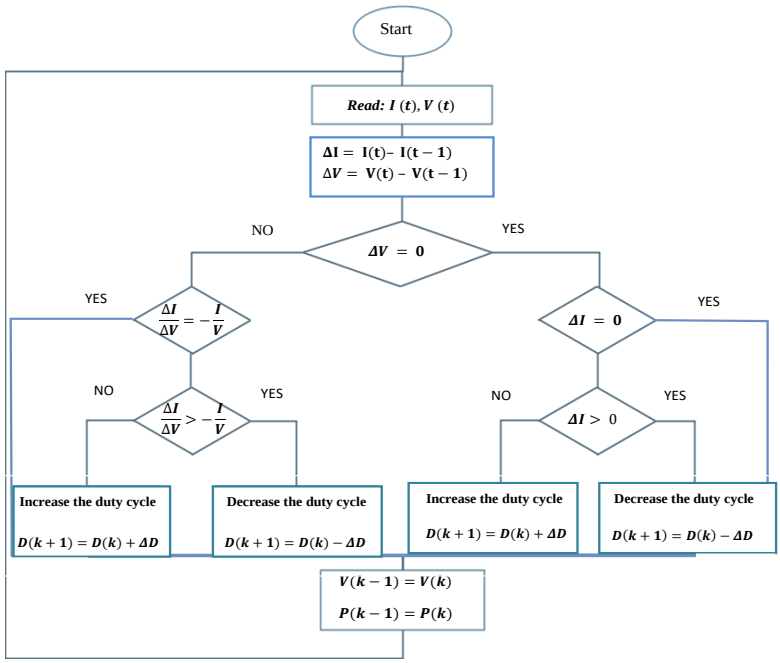

Fig. 11. Flowchart of the IncCond MPPT method.

C. *Fuzzy Logic-Based MPPT Control*

This approach is based on two essential concepts: that of the decomposition of a range of variations of a variable in the form of linguistic nuances: “low”, “medium”, “high” ... and rules coming from the expertise of the human operator, which express, in linguistic form, how the system controls must evolve according to the observed variables:

“If the error is positively large and the variation of the error is positively large, then the variation of the output is very negative”.

Figure 12 shows the proposed configuration of the fuzzy logic controller. The scaling factors $\boldsymbol{E}$ and $\Delta\boldsymbol{D}$ cause the input and output values of the controller to change proportionally.

In the fuzzification phase, the actual voltage and current of the photovoltaic generator are measured instantly, and the power can be calculated as follows

$$\boldsymbol{P}(\boldsymbol{k}) = \boldsymbol{I}(\boldsymbol{k}) \times \boldsymbol{V}(\boldsymbol{k}). \tag{8}$$

The error (E) and the change in error (ΔE) at the sampled times (k) are expressed as

$$\boldsymbol{E}(\boldsymbol{k}) = \frac{\boldsymbol{P}(\boldsymbol{k}) - \boldsymbol{P}(\boldsymbol{k}-\boldsymbol{1})}{\boldsymbol{V}(\boldsymbol{k}) - \boldsymbol{V}(\boldsymbol{k}-\boldsymbol{1})} \tag{9}$$

and

$$\boldsymbol{\Delta E} = \boldsymbol{E}(\boldsymbol{k}) - \boldsymbol{E}(\boldsymbol{k}-\boldsymbol{1}). \tag{10}$$

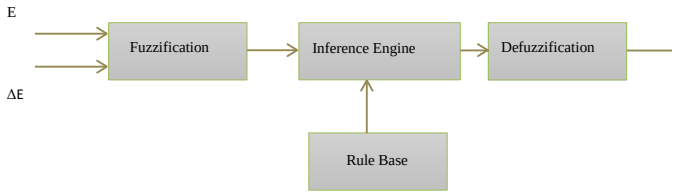

Fig. 12. Principle of MPPT with the FLC method.

The rule base is made up of the rules shown in Table II. As an explicative example, the rule:

"*If E is Big and ΔE is Z then ΔD is S*" means that:

"If the operating point is far from the maximum power point toward the left side, and the change in the slope of the P-V curve is approximately zero; then reduce the duty cycle slightly".

TABLE II. RULES BASE IN THE FLC TO INFER ΔD.

E / ΔE	Very Small	Small	Zero	Big	Very Big
Very Small	VB	VB	VB	B	B
Small	VB	B	B	B	Z
Zero	Z	Z	Z	Z	Z
Big	VS	VS	S	S	Z
Very Big	VS	VS	VS	S	S

For a sampled data representation in the defuzzification phase, the centre of gravity is calculated by

$$\boldsymbol{\Delta D} = \frac{\sum_{j=1}^{n} \boldsymbol{\mu}(\boldsymbol{D}_j) - \boldsymbol{D}_j}{\sum_{j=1}^{n} \boldsymbol{\mu}(\boldsymbol{D}_j)}. \tag{11}$$

The output variable (ΔD) is the increment step of the duty cycle, which can take positive or negative values depending on the location of the operating point. This output is sent to the DC-DC converter to drive the load. Using the value of ΔD provided by the controller, an accumulator was created to obtain the duty cycle value

$$\boldsymbol{D} = \boldsymbol{D}(\boldsymbol{k}-\boldsymbol{1}) + \boldsymbol{\Delta D}(\boldsymbol{k}). \tag{12}$$

D. Comparison of the Results

A series of simulations have been carried out for the three techniques under different environmental conditions to draw a detailed comparison using zeta converter.

Figures 13 and 14 show the performance of the three methods in terms of meeting the power required by the greenhouse and the variations in the duty ratio under constant irradiance and temperature. It is observed that the three methods could attain the final power value at almost the same response time (t_r = 0.022 s). FLC shows less ripple (<1 W) than the other two methods (up to 1 W for P&O). Variations in the duty ratio are also less in the FLC.

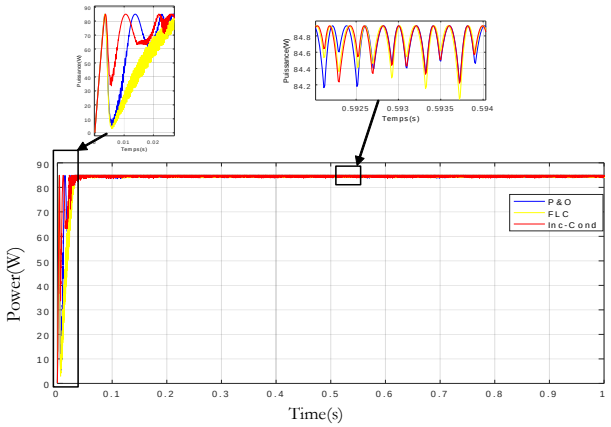

Fig. 13. Variations of PV panel power in the three MPPT techniques, P&O, IncCond, and FLC, under constant operating conditions: T = 45 °C and E = 1000 W/m².

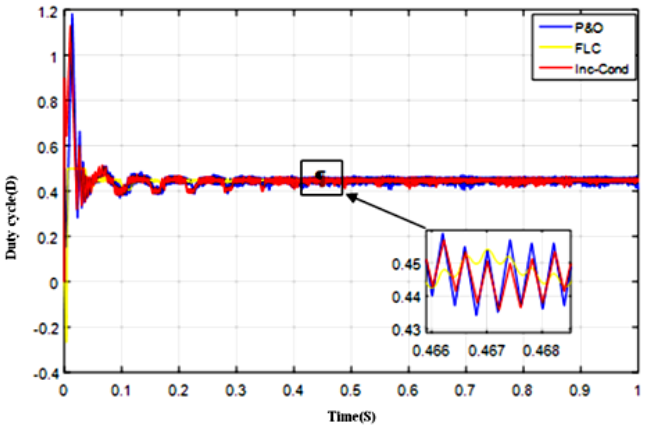

Fig. 14. Variations in the duty ratio for the three MPPT techniques, P&O, IncCond, and FLC, under constant operating conditions: T = 45 °C and E = 1000 W/m².

Figures 15–18 illustrate the PVG power response of the three techniques under different operating conditions. Table III provides a summary of the performance parameters of each algorithm under simultaneous abrupt changes in irradiation and temperature. Here, the classical methods P&O and IncCond show better results especially for the response time. However, there is a small change in the values of the duty ratio, but the IncCond technique shows slightly higher overshoot as compared to the other two methods.

TABLE III. PERFORMANCE PARAMETERS COMPARISON IN THE THREE TECHNIQUES.

Method	Sampling time	Response time t_r(s)	Stability	Duty ratio
P&O	0.001	0.022	Oscillates	[.413 .467]
IncCond	0.001	0.0225	Oscillates	[.423 .46]
FLC	Variable	0.323	Oscillates	[.435 .46]

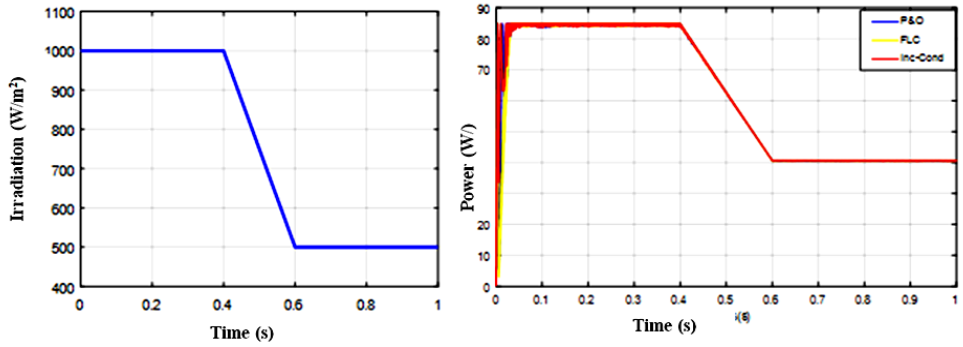

Fig. 15. PVG output power response of the three algorithms under slow change in the irradiation.

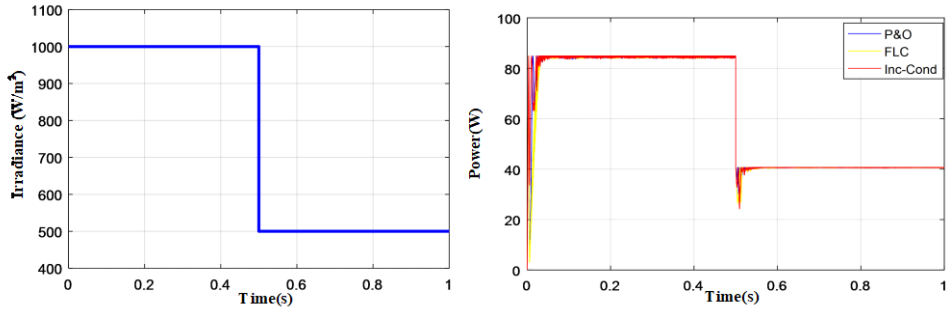

Fig. 16. PVG output power response of the three algorithms under abrupt change in irradiation.

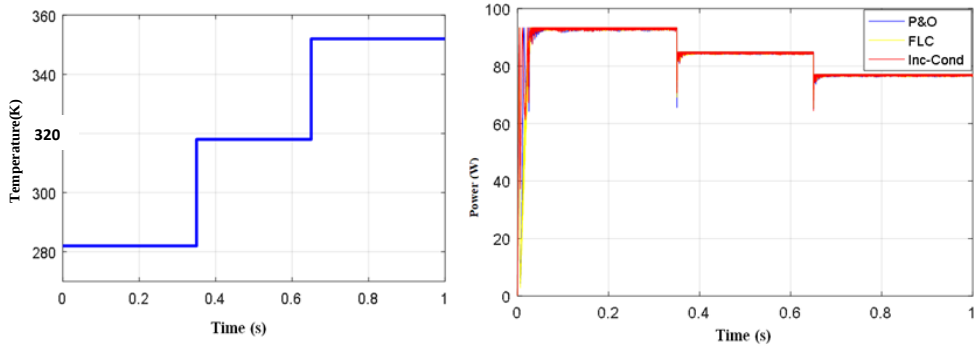

Fig. 17. PVG output power response of the three algorithms under temperature changes.

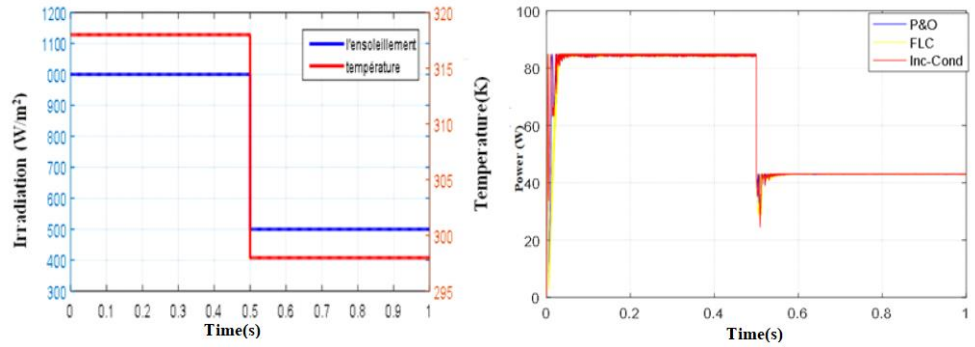

Fig. 18. PVG output power response of the three algorithms under simultaneous abrupt changes in irradiation and temperature.

E. Comparison of Converters

Figures 19–22 give the power and voltage responses of the two converters separately using the three MPPT algorithms operating under different environmental conditions. We note that the response time of the PVG power in the constant conditions of P&O and IncCond for the buck-boost is 0.06 s and 0.02 s for the Zeta. Also, the output voltage ripple of the Zeta converter is less than that of the buck-boost converter.

The Zeta converter outperforms the buck-boost in all aspects and for each control technique. However, if there are no sensitive devices in the greenhouse (e.g., high-precision transducers) the use of buck-boost converter is preferred, because of its low cost and simplicity as compared to the Zeta topology.

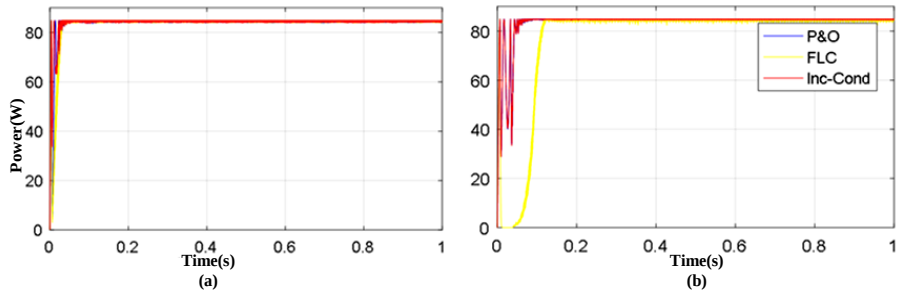

Fig. 19. PVG power response for the three MPPTs techniques under constant operating conditions using: (a) ZETA converter; (b) Buck-boost converter.

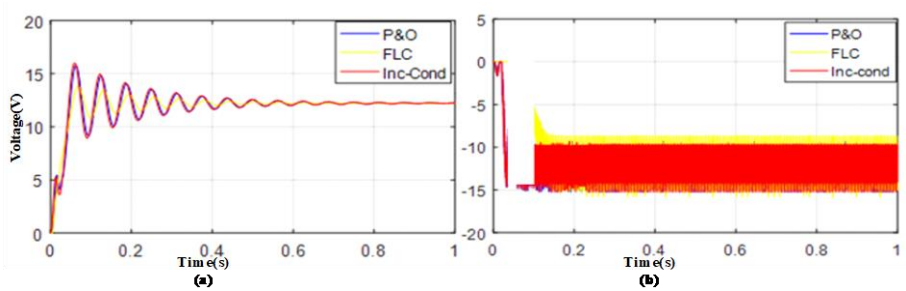

Fig. 20. PVG output voltage response for the three MPPT techniques under constant operating conditions using: (a) ZETA converter; (b) Buck-boost converter.

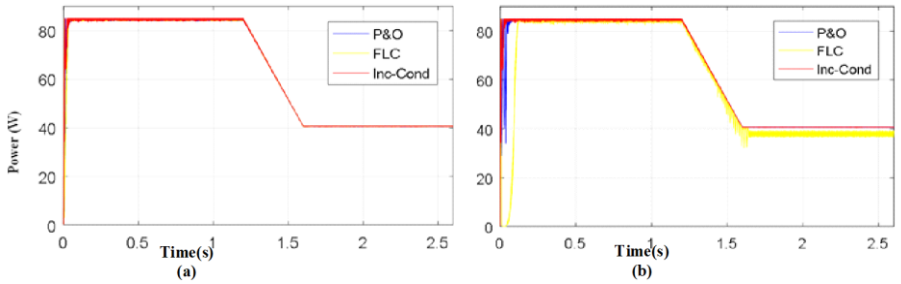

Fig. 21. PVG power response for the three MPPT techniques under slow change in irradiation using: (a) ZETA converter; (b) Buck-boost converter.

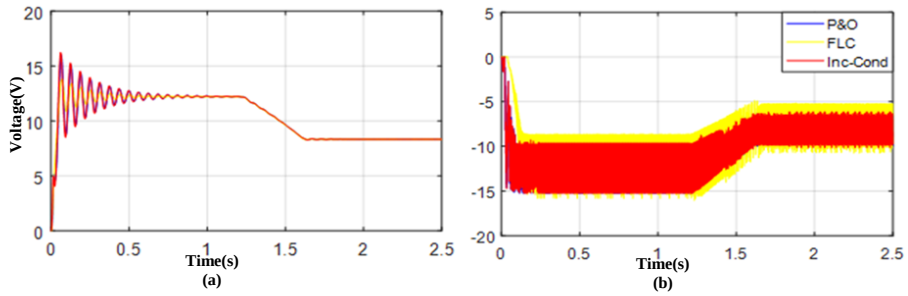

Fig. 22. PVG output voltage response for the three MPPT techniques under slow change in irradiation using: (a) Zeta converter; (b) Buck-boost converter.

In a gros-au-modo, the two converters could provide the required maximum power required by the smart greenhouse using either control algorithm. However, for precise output voltage, specifically for highly sensitive transducers and sensors, the use of Zeta converter is favoured.

V. CONCLUSIONS

A two-tier comparison study was carried out to evaluate the performance of P&O, IncCond, and FLC-based MPPT algorithms applied to two types of DC converters powered by a photovoltaic generator to power a remote standalone smart greenhouse. The energy chain consisted of the PVG, the adaptation stage based on the maximum power point tracking technique (MPPT), and the load (greenhouse). The Zeta converter was in the adaptation stage at first and then it was replaced by buck-boost converter.

The tracking mechanism to extract maximum power under different operating conditions has been established using the three MPPT methods based on power feedback.

The maximum power was achieved in the three control methods and for the two converters, even during variable environmental conditions (irradiation and temperature). The P&O and IncCond methods show better results, especially for the response time under stable conditions for the Zeta converter. However, there was a small change in the values of the duty ratio, but the IncCond technique shows a slightly higher overshoot as compared to the other two methods.

The Zeta converter surpassed the buck-boost in all aspects and for each control technique. However, if there are no sensitive devices in the greenhouse (e.g., high-precision transducers), the use of buck-boost converter is preferred due to its low cost and simplicity as compared to the Zeta topology.

In general, the two converters could provide the maximum

power required by the smart greenhouse using either control algorithm. However, for precise output voltage, specifically for high sensitive transducers and sensors, the use of a Zeta converter is favoured.

CONFLICTS OF INTEREST

The authors declare that they have no conflicts of interest.

REFERENCES

[1] K. Gairaa and Y. Bakelli, "Solar energy potential assessment in the Algerian south area: Case of Ghardaïa region", *Journal of Renewable Energy*, vol. 2013, art. 496348, pp. 1–11, 2023. DOI: 10.1155/2013/496348.

[2] J. Chen, J. Yang, J. Zhao, F. Xu, Z. Shen, and L. Zhang, "Energy demand forecasting of the greenhouses using nonlinear models based on model optimized prediction method", *Neurocomputing*, vol. 174, part B, pp. 1087–1100, 2016. DOI: 10.1016/j.neucom.2015.09.105.

[3] O. Bouketir, "An automatic irrigation system for water optimization in the Algerian agricultural sector", *Agricultural Science and Technology*, vol. 11, no. 2, pp. 133–137, 2019. DOI: 10.15547/ast.2019.02.021.

[4] O. Bouketir and Y. Boukazoul, "A multi-sensor farming prototype system for growing tomato in Algeria", in *Proc. of 19th International Multi-Conference on Systems, Signals & Devices (SSD)*, 2022, pp. 1929–1935. DOI: 10.1109/SSD54932.2022.9955729.

[5] E. Iddio, L. Wang, Y. Thomas, G. McMorrow, and A. Denzer, "Energy efficient operation and modeling for greenhouses: A literature review", *Renewable and Sustainable Energy Reviews*, vol. 117, art. 109480, 2020. DOI: 10.1016/j.rser.2019.109480.

[6] A. Soussi, E. Zero, A. Ouammi, D. Zejli, S. Zahmoun, and R. Sacile, "Greenhouse towards near zero energy consumption: Challenges, opportunities, and future directions", *Preprints*, 2023. DOI: 10.20944/preprints202308.0451.v1.

[7] Y. Shen, R. Wei, and L. Xu, "Energy consumption prediction of a greenhouse and optimization of daily average temperature", *Energies*, vol. 11, no. 1, p. 65, 2018. DOI: 10.3390/en11010065.

[8] F. Liu, S. Duan, F. Liu, B. Liu, and Y. Kang, "A variable step size INC MPPT method for PV systems", *IEEE Trans. Indus. Elect.*, vol. 55, no. 7, pp. 2622–2628, 2008. DOI: 10.1109/TIE.2008.920550.

[9] A. Ali *et al.*, "Investigation of MPPT techniques under uniform and non-uniform solar irradiation condition–A retrospection", *IEEE Access*, vol. 8, pp. 127368–127392, 2020. DOI: 10.1109/ACCESS.2020.3007710.

[10] Z. Fan, S. Li, H. Cheng, and L. Liu, "Perturb and observe MPPT algorithm of photovoltaic system: A review", in *Proc. of 33rd Chinese Control and Decision Conference (CCDC)*, 2021, pp. 1413–1418. DOI: 10.1109/CCDC52312.2021.9602272.

[11] A. M. Eltamaly, "Chapter 4 - Performance of MPPT techniques of photovoltaic systems under normal and partial shading conditions", *Advances in Renewable Energies and Power Technologies*, vol. 1: Solar and Wind Energies, pp. 115–161, 2018. DOI: 10.1016/B978-0-12-812959-3.00004-6.

[12] A. S. Mahdi, A. K. Mahamad, S. Saon, T. Tuwoso, H. Elmunsyah, and S. W. Mudjanarko, "Maximum power point tracking using perturb and observe, fuzzy logic and ANFIS", *SN Appl. Sci*., vol. 2, no. 1, p. 89, 2020. DOI: 10.1007/s42452-019-1886-1.

[13] L. Shang, H. Guo, and W. Zhu, "An improved MPPT control strategy based on incremental conductance algorithm", *Prot. Control Mod. Power Syst*., vol. 5, art. no. 14, 2020. DOI: 10.1186/s41601-020-00161-z.

[14] M. H. Ibrahim, S. P. Ang, M. N. Dani, M. I. Rahman, R. Petra, and S. M. Sulthan, "Optimizing step-size of perturb & observe and incremental conductance MPPT techniques using PSO for grid-tied PV system", *IEEE Access*, vol. 11, pp. 13079–13090, 2023. DOI: 10.1109/ACCESS.2023.3242979.

[15] U. Prasatsap, N. Nernchad, C. Termritthikun, S. Srita, T. Kaewchum, and S. Somkun, "Comparison of control configurations and MPPT algorithms for single-phase grid-connected photovoltaic inverter", *Advances in Electrical and Computer Engineering*, vol. 23, no. 2, pp. 55–66, 2023. DOI: 10.4316/AECE.2023.02007.

[16] A. Durusu, I. Nakir, A. Ajder, R. Ayaz, H. Akca, and M. Tanrioven, "Performance comparison of widely-used maximum power point tracker algorithms under real environmental conditions", *Advances in Electrical and Computer Engineering*, vol. 14, no. 3, pp. 89–94, 2014. DOI: 10.4316/AECE.2014.03011.

[17] A. K. Gupta *et al.*, "Effect of various incremental conductance MPPT methods on the charging of battery load feed by solar panel", *IEEE Access*, vol. 9, pp. 90977–90988, 2021. DOI: 10.1109/ACCESS.2021.3091502.

[18] J. Ingilala and I. Vairavasundaram, "Investigation of high gain DC/DC converter for solar PV applications", *e-Prime - Advances in Electrical Engineering, Electronics and Energy*, vol. 5, art. 100264, 2023. DOI: 10.1016/j.prime.2023.100264.

[19] T. Sutikno, A. S. Samosir, R. A. Aprilianto, H. S. Purnama, W. Arsadiando, and S. Padmanaban, "Advanced DC–DC converter topologies for solar energy harvesting applications: A review", *Clean Energy*, vol. 7. no. 3, pp. 555–570, 2023. DOI: 10.1093/ce/zkad003.

[20] L. Song, S. Duan, T. Wang, and X. Liu, "A simplified flying capacitor voltage control strategy for hybrid clamped three-level boost converter in photovoltaic system", *IEEE Trans. Indus. Elect.*, vol. 69, no. 8, pp. 8004–8014, 2022. DOI: 10.1109/TIE.2021.3104607.

[21] K. A. M. Junaid *et al.*, "PV-based DC-DC buck-boost converter for LED driver", *e-Prime - Advances in Electrical Engineering, Electronics and Energy*, vol. 5, art. 100271, 2023. DOI: 10.1016/j.prime.2023.100271.

[22] R. Rahimi, S. Habibi, M. Ferdowsi, and P. Shamsi, "Z-source-based high step-up DC–DC converters for photovoltaic applications", *IEEE Journal of Emerging and Selected Topics in Power Electronics*, vol. 10, no. 4, pp. 4783–4796, 2022. DOI: 10.1109/JESTPE.2021.3131996.

[23] M. I. S. Guerra, F. M. Ugulino de Araújo, M. Dhimish, and R. G. Vieira, "Assessing maximum power point tracking intelligent techniques on a PV system with a buck–boost converter", *Energies*, vol. 14, no. 22, p. 7453, 2021. DOI: 10.3390/en14227453.

[24] A. Pradhan and B. Panda, "Design of DC-DC converter for load matching in case of PV system", in *Proc. of International Conference on Energy, Communication, Data Analytics and Soft Computing (ICECDS)*, 2017, pp. 1002–1007. DOI: 10.1109/ICECDS.2017.8389588.

[25] A. Escamilla-García, G. M. Soto-Zarazúa, M. Toledano-Ayala, E. Rivas-Araiza, and A. Gastélum-Barrios, "Applications of artificial neural networks in greenhouse technology and overview for smart agriculture development", *Appl. Sci.*, vol. 10, no. 11, p. 3835, 2020. DOI: 10.3390/app10113835.

[26] M. C. Bozchalui, C. A. Cañizares, and K. Bhattacharya, "Optimal energy management of greenhouses in smart grids", *IEEE Trans. Smart Grid*, vol. 6, no. 2, pp. 827–835, 2015. DOI: 10.1109/TSG.2014.2372812.

[27] S. Hemming *et al.*, "Innovations in greenhouse systems—Energy conservation by system design, sensors and decision support systems", in *Proc. of the International Symposium on New Technologies and Management for Greenhouses - GreenSys 2015*, 2017, pp. 1–15. DOI: 10.17660/ActaHortic.2017.1170.1.

[28] W. Issaadi, A. Khireddine, and S. Issaadi, "Management of a base station of a mobile network using a photovoltaic system", *Renewable and Sustainable Energy Reviews*, vol. 59, pp. 1570–1590, 2016. DOI: 10.1016/j.rser.2015.12.054.

[29] H. Saber, A. E. Bendaouad, L. Rahmani, and H. Radjeai, "A comparative study of the FLC, INC and P&O methods of the MPPT algorithm for a PV system", in *Proc. of 2022 19th International Multi-Conference on Systems, Signals & Devices (SSD)*, 2022, pp. 2010–2015. DOI: 10.1109/SSD54932.2022.9955905.

[30] J. L. Seguel, S. I. Seleme, and L. M. F. Morais, "Comparative study of buck-boost, SEPIC, Cuk and Zeta DC-DC converters using different MPPT methods for photovoltaic applications", *Energies*, vol. 15, no. 21, p. 7936, 2022. DOI: 10.3390/en15217936.